

## Thermal properties of rare earth dodecaborides

Andrzej Czopnik,<sup>a,\*</sup> Nataly Shitsevalova,<sup>a,b</sup> Alexander Krivchikov,<sup>a,c</sup> Vasyly Pluzhnikov,<sup>a,c</sup>  
Yuriy Paderno,<sup>b</sup> and Yoshichika Ōnuki<sup>d</sup>

<sup>a</sup> *W. Trzebiatowski Institute of Low Temperature and Structure Research of PAS, P.O. Box 1410, 50-950 Wrocław, Poland*

<sup>b</sup> *I. Frantsevich Institute for Problems of Materials Science of NASU, 03680 Kiev, Ukraine*

<sup>c</sup> *B. Verkin Institute for Low Temperature Physics and Engineering of NASU, Kharkiv 61103, Ukraine*

<sup>d</sup> *Graduate School of Science, Osaka University, Toyonaka 560-0810, Japan*

Received 14 October 2002; received in revised form 18 December 2002; accepted 29 April 2003

### Abstract

We have measured heat capacity and thermal expansion of rare earth dodecaborides  $REB_{12}$  ( $RE = Y, Tb-Tm, Lu$ ).  $YB_{12}$  and  $LuB_{12}$  are diamagnetics whereas the other dodecaborides are ordered antiferromagnetically. The amplitude of the heat capacity discontinuity at the Néel temperature and the shape of the heat capacity variation in the critical region for all these antiferromagnetics are characteristics for amplitude-modulated magnetic structures. In the ordered state  $TbB_{12}$  reveals two first-order phase transitions, most likely due to magnetic structure changes. The heat capacity of  $ErB_{12}$  just below the Néel point shows an anomaly of unclear origin. From the Schottky contribution to the heat capacity we have determined crystal field parameters. They are completely different than that is estimated from Point Charge Model.

© 2003 Elsevier Inc. All rights reserved.

**Keywords:** Rare earth dodecaborides; Heat capacity; Thermal expansion; Crystal electric field; Amplitude-modulated magnetic structure

### 1. Introduction

All rare earth dodecaborides, except  $ScB_{12}$ , crystallize in a face-centered cubic structure of the  $UB_{12}$ -type (sp.gr.  $Fm\bar{3}m-O_h^5$ ), which may be considered as a simple closest-packed lattice formed by rigid units- $B_{12}$  cubooctahedrons with metal atoms located in cavities of this lattice. The crystal structure may also be deduced from the NaCl-type structure, where the Na-sites are occupied by  $RE$ -ions and the Cl-sites by  $B_{12}$  cubooctahedrons [1]. In this structure  $RE$ -ions form a *fcc* lattice.

Strong covalent bonds between boron atoms intra and inter  $B_{12}$  cages lead to very rigid boron sublattice. To compensate for the electron deficiency in the boron sublattice in order to reach the maximum stability two valence electrons per each rare earth atom are transferred to this sublattice. In three-valent rare earth dodecaborides the third valence electron enters the conduction band. So all dodecaborides studied in this

work are good metals, in which conduction bands at the Fermi level have mainly a  $RE$   $5d$ -character with an admixture of  $B$   $2p$  [2,3]. As a consequence, an exchange interaction between spins of the  $4f$ -shells is of the RKKY-type, which leads to the antiferromagnetic ordering [4–6] in  $TbB_{12}$ ,  $DyB_{12}$ ,  $HoB_{12}$ ,  $ErB_{12}$ , and  $TmB_{12}$  with Néel temperatures equal to 22.05, 16.35, 7.38, 6.65 and 3.28 K, respectively. Diamagnetic  $LuB_{12}$  is a superconductor below 0.5 K [7].

On the ground of  $^{169}Tm$  Mössbauer spectroscopy Gubbens et al. [8] have concluded that  $TmB_{12}$  is a crystal field (CF) singlet–triplet system, so the antiferromagnetic ordering is the result of induced magnetic moment into the ground state by closely spaced ( $\Delta = 6 \pm 2$  K)  $\Gamma_4$  triplet. The same CF ground state and overall CF splitting gives the Point Charge Model (PCM) ( $W = -0.144$  K,  $x = -0.97$ ) within the LLW parameterization scheme [9]. However, our studies of Schottky heat capacity yield  $W = 1.09$  K and  $x = -0.15$  and consequently the magnetic ground state  $\Gamma_5^{(1)}$  [10]. The recently determined CF-parameters ( $W = 1.19$  K and  $x = -0.074$ ) by inelastic neutron scattering are in good agreement with them. Therefore one may reject the

\*Corresponding author. Fax: 380-44-444-31-21.

E-mail address: [shitz@ipms.kiev.ua](mailto:shitz@ipms.kiev.ua), [czopnik@int.pan.wroc.pl](mailto:czopnik@int.pan.wroc.pl) (A. Czopnik).

supposition on induced type of antiferromagnetism in  $\text{TmB}_{12}$  [10].

Among the dodecaborides a magnetic structure has been determined only for  $\text{TmB}_{12}$  [10] and  $\text{TbB}_{12}$  [11]. The magnetic structure of both compounds below the Néel temperature is a sinusoidally modulated one. The propagation vector is equal to  $\mathbf{k} = (1/2 \pm \tau, 1/2 \pm \tau, 1/2 \pm \tau)$ . The structure can be described as a modulation of magnetic moments (stacked parallel in (111) sheets but with antiparallel orientation of the neighboring sheets) which propagates along three crystallographic directions.

Except  $\text{TmB}_{12}$  [12] there is no direct information from inelastic neutron scattering on CEF-splitting in rare earth dodecaborides. Without this knowledge it is impossible to analyze quantitatively their physical properties. On the other hand low-temperature thermal properties such as a heat capacity as well as thermal expansion may serve as probes for crystal field determination. So we have undertaken this work, first of all, for the determination of crystal field parameters. However, this study may give also important information on magnetic ordering in rare earth dodecaborides. Blanco et al. in a series of papers [13–16] have shown that within the Periodic Field Model (PFM) the heat capacity behavior in the critical region of an antiferromagnetic transition is distinctly different for systems with amplitude-modulated (AM) magnetic structure in comparison to systems with equal moment (EM) magnetic structures.

## 2. Experimental details

We used high-purity  $\text{TbB}_{12}$  sintered samples and  $\text{DyB}_{12}$ ,  $\text{HoB}_{12}$ ,  $\text{ErB}_{12}$ ,  $\text{TmB}_{12}$ ,  $\text{LuB}_{12}$  single crystals grown by the crucible free inductive zone melting process in an atmosphere of pure argon. The details of sample preparation are described in Ref. [17].

The heat capacity ( $C_p$ ) was measured by a pulse quasi-adiabatic method between 2.6 and 70 K using a calorimeter the details of which are described in Ref. [18]. Mass of the studied samples was no more than 750 mg. The calorimeter measures the heat capacity in comparison to the standard heat capacity data of copper with an error  $\pm 1\%$  in the whole temperature range. The heat capacity of  $\text{ErB}_{12}$ ,  $\text{TmB}_{12}$  and  $\text{LuB}_{12}$  in the temperature range 0.5–2.6 K was measured by using a similar method in Osaka University.

The temperature dependence of a relative length change ( $\Delta L/L$ ) was measured in the range 5–200 K with a resolution of  $1 \times 10^{-9}$  by a three-terminal capacitance method. The used capacitance cell was similar to that described by Brandli and Griessen [19]. The thermal expansion of the investigated sample  $\Delta L/L$  was approximated by cubic splines after subtraction of

the cell contribution. Then the linear thermal expansion coefficient  $\alpha = (\partial \ln Z / \partial T)_p$  was easily determined. The relative experimental error  $\Delta L/L$  by standard copper is no more than  $\pm 1\%$  below 20 K and decreases down to 0.3% near 200 K. The samples were cylinders or parallelepipeds ( $L = 4\text{--}6$  mm) with plane-parallel basis (precision  $\pm 1 \mu$ ).

## 3. Results and discussion

### 3.1. Heat capacity

Temperature dependencies of the heat capacity of all studied dodecaborides are shown in Fig. 1 in log-log scale. The heat capacity of  $\text{TbB}_{12}$  and  $\text{ErB}_{12}$  in the ordered range is shown in Fig. 2. The observed behavior of the heat capacity in the critical region of all antiferromagnetic dodecaborides is intrinsic for amplitude-modulated magnetic systems. Namely, (1) the heat capacity maximum ( $T_M$ ) lies below the Néel temperature ( $T_N$ ) determined from the magnetic susceptibility (Table 1) and (2). As we show later in this paper the heat capacity at  $T_M$  is equal to that expected for amplitude-modulated magnetic systems. In the ordered state  $\text{TbB}_{12}$  reveals two first-order transitions due to magnetic structure changes [11]. Just below the Néel temperature  $\text{ErB}_{12}$  shows a small anomaly of unclear origin.

Our recent neutron diffraction studies have shown that  $\text{TmB}_{12}$  [10] and  $\text{TbB}_{12}$  [11] indeed order within sinusoidally modulated magnetic structures. Magnetic structure of terbium dodecaboride remains modulated down to 4 K the lowest temperature, at which the neutron scattering experiment has been performed.

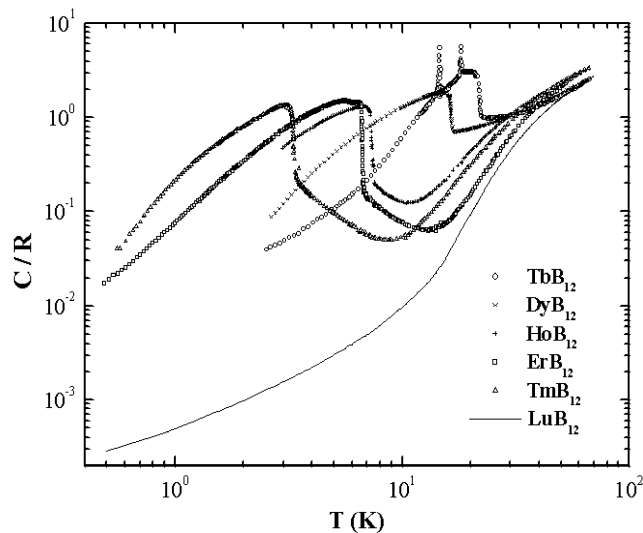


Fig. 1. Temperature dependence of the heat capacity of rare earth dodecaborides.

It is well known that only if the crystal field ground state is a nonmagnetic state or a many-body singlet (attributed to Kondo effects) the modulated magnetic structure can remain stable down to 0 K. In the opposite case, due to entropy effects associated with the modulation of the magnetic moment amplitude, the magnetic system should either (1) suddenly jump through a first-order transition to an equal magnetic moment structure

or (2) evolve to an antiphase structure at 0 K through a progressive squaring up of the modulation. This latter process is accompanied by growing of higher order harmonics of the propagation vector.

We emphasize, in order to understand the observed behavior as well as other physical properties of the dodecaborides we have to know their crystal field. Because of the lack of this information from direct experiment, i.e. inelastic neutron scattering, we tried to determine CF-parameters from Schottky contribution to entropy ( $S$ ) and heat capacity ( $C_{\text{Sch}}$ ):

$$S = -\left(\frac{\partial F}{\partial T}\right) = R(\ln Z + \langle E \rangle / k_B T), \quad (1)$$

$$C_{\text{Sch}} = -T\left(\frac{\partial^2 F}{\partial T^2}\right) = \frac{R}{k_B^2 T^2}(\langle E^2 \rangle - \langle E \rangle^2), \quad (2)$$

where  $\langle X \rangle = \frac{\sum_{i=1}^n f_i X_i \exp(-E_i/k_B T)}{\sum_{i=1}^n f_i \exp(-E_i/k_B T)}$ —statistical average;  $Z = \sum_{i=1}^n f_i \exp(-E_i/k_B T)$ —partition function;  $F$ —Helmholtz free energy;  $E_i$ —energy of CEF level with degeneracy  $f_i$ .

In order to extract a magnetic contribution  $C_m$  from the full heat capacity  $C_p$  of the magnetic dodecaborides we use the heat capacity of nonmagnetic reference compound  $\text{LuB}_{12}$  as a sum of electronic and lattice contribution to the total heat capacity. The heat capacity of  $\text{LuB}_{12}$  is characterized by Sommerfeld coefficient  $\gamma = 4.14 \pm 0.02 \text{ mJ}/(\text{mol K}^2)$  and Debye temperature  $\Theta_D = 1110 \pm 80 \text{ K}$ . In further analysis we neglect the electronic heat capacity because it yields the main contribution to  $C_p$  in the low temperature range (up to 10 K), where the magnetic part is several orders of magnitude greater than  $C_p$  of  $\text{LuB}_{12}$ .

Next, because of a difference in molar masses of the studied compounds we should appropriately renormalize the heat capacity of  $\text{LuB}_{12}$

$$C_{\text{ph}}(\text{REB}_{12}) = k C_p(\text{LuB}_{12}). \quad (3)$$

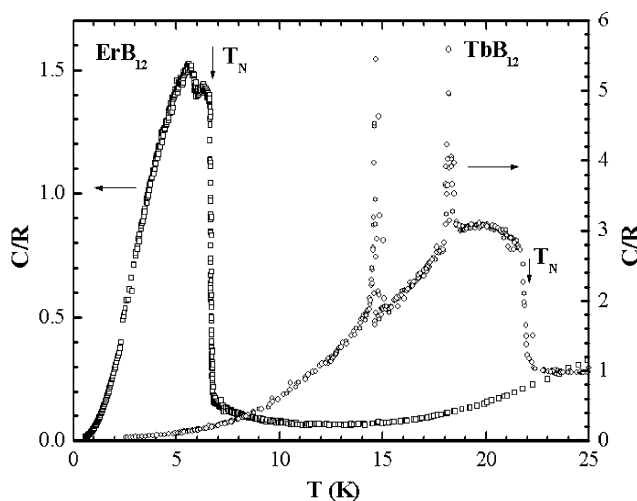


Fig. 2. Temperature dependencies of the  $\text{TbB}_{12}$  and  $\text{ErB}_{12}$  heat capacities in expanded low-temperature range.

Table 1  
The temperatures of the  $\text{REB}_{12}$  phase transitions

$\text{REB}_{12}$	$T_M$ (K)	$T_N(\chi)$ (K) [6]	Remarks
$\text{TbB}_{12}$	19.87	22.05	Two phase transitions of the first-order at 18.19 and 14.61 K
$\text{DyB}_{12}$	15.20	16.35	
$\text{HoB}_{12}$	6.61	7.38	
$\text{ErB}_{12}$	6.38	6.65	Anomaly at 5.59 K
$\text{TmB}_{12}$	3.08	3.28	

Table 2  
The schemes of the splitting of the RE-ions ground multiplet by  $\text{REB}_{12}$  crystal electric field

$\text{TbB}_{12}$		$\text{DyB}_{12}$		$\text{HoB}_{12}$		$\text{ErB}_{12}$		$\text{TmB}_{12}$					
I	II	I	II	I	I	I	I	I	I				
$W = -0.38 \text{ K}$ $x = 0.44$	$W = -0.29 \text{ K}$ $x = -0.017$	$W = -0.18 \text{ K}$ $x = 0.66$	$W = 3.92 \text{ K}$ $x = -0.47$	$W = 0.73 \text{ K}$ $x = 0.42$	$W = -0.85 \text{ K}$ $x = 0.37$	$W = -0.85 \text{ K}$ $x = 0.37$	$W = -0.85 \text{ K}$ $x = 0.37$	$W = 1.25 \text{ K}$ $x = -0.12$	$W = 1.25 \text{ K}$ $x = -0.12$				
$\Gamma_i$	$E_i$ (K)	$\Gamma_i$	$E_i$ (K)	$\Gamma_i$	$E_i$ (K)	$\Gamma_i$	$E_i$ (K)	$\Gamma_i$	$E_i$ (K)	$\Gamma_i$	$E_i$ (K)	$\Gamma_i$	$E_i$ (K)
$\Gamma_2$	0	$\Gamma_2$	0	$\Gamma_8^{(3)}$	0	$\Gamma_7$	0	$\Gamma_5^{(1)}$	0	$\Gamma_8^{(3)}$	0	$\Gamma_5^{(1)}$	0
$\Gamma_5^{(2)}$	20.6	$\Gamma_5^{(2)}$	24.1	$\Gamma_6$	7.1	$\Gamma_6$	24.7	$\Gamma_3^{(1)}$	63.3	$\Gamma_6$	115.0	$\Gamma_3$	78.7
$\Gamma_3$	39.7	$\Gamma_1$	45.2	$\Gamma_8^{(2)}$	54.3	$\Gamma_8^{(1)}$	75.3	$\Gamma_4^{(1)}$	135.0	$\Gamma_8^{(2)}$	217.0	$\Gamma_4$	170.0
$\Gamma_4$	62.6	$\Gamma_4$	47.7	$\Gamma_7$	61.4	$\Gamma_8^{(2)}$	1182	$\Gamma_5^{(2)}$	149.0	$\Gamma_8^{(1)}$	288.0	$\Gamma_1$	183.0
$\Gamma_1$	65.9	$\Gamma_3$	64.9	$\Gamma_8^{(1)}$	68.2	$\Gamma_8^{(3)}$	1227	$\Gamma_1$	284.0	$\Gamma_7$	360.0	$\Gamma_5^{(2)}$	243.0
$\Gamma_5^{(1)}$	78.1	$\Gamma_5^{(1)}$	88.6					$\Gamma_4^{(2)}$	393.0			$\Gamma_2$	329.0
								$\Gamma_3^{(2)}$	416.0				

We accept the most frequently used expression for the renormalization factor  $k$ :

$$k = \frac{C_{\text{ph}}(\text{REB}_{12})}{C_{\text{ph}}(\text{LuB}_{12})} = \left( \frac{\Theta_{\text{D}}(\text{LuB}_{12})}{\Theta_{\text{D}}(\text{REB}_{12})} \right)^3 = \left( \frac{M(\text{REB}_{12})}{M(\text{LuB}_{12})} \right)^{3/2}, \quad (4)$$

where  $\Theta_{\text{D}}$ —Debye temperature,  $M$ —molar mass.

The calculated  $k$  values for  $\text{TbB}_{12}$ ,  $\text{DyB}_{12}$ ,  $\text{HoB}_{12}$ ,  $\text{ErB}_{12}$  and  $\text{TmB}_{12}$  are equal to 0.921, 0.938, 0.950, 0.962 and 0.970, respectively. Now we can analyze CF contribution to the heat capacity of dodecaborides. In Fig. 3 this analysis is shown for  $\text{TbB}_{12}$ . Best agreement between the experimental Schottky contribution and calculated one we obtained for two sets of CF parameters: (1)  $W = -0.38$  K,  $x = 0.44$  and (2)  $W = -0.29$  K,  $x = -0.017$ . Both sets give the singlet  $\Gamma_2$  as the ground state and the triplet  $\Gamma_5^{(2)}$ —as the first excited level (Table 2). For both CF parameter sets the overall CF-splitting is rather small and does not exceed 90 K. However, the magnetic entropy calculated for these parameters exceeds clearly the experimentally determined one  $S_{\text{m}}$  (insert in Fig. 3).

Similar situation as in the case of  $\text{TbB}_{12}$ , we found for  $\text{DyB}_{12}$  (Fig. 4). Here also for two sets of CF-parameters—(1)  $W = -0.18$  K,  $x = 0.66$  and (2)  $W = 3.92$  K,  $x = -0.47$ —the calculated Schottky heat capacity ( $C_{\text{Sch}}$ ) agrees quite well with the experimental one but calculated entropy disagrees with the experimentally determined one (insert in Fig. 4). At the Néel temperature the experimental  $S_{\text{m}}$  reaches  $R \ln 4$ . Thus the ground state should be either a quartet, or a pseudo-quartet.

The failure in univocal determination of CF-parameters for these two compounds is, first of all, due to the

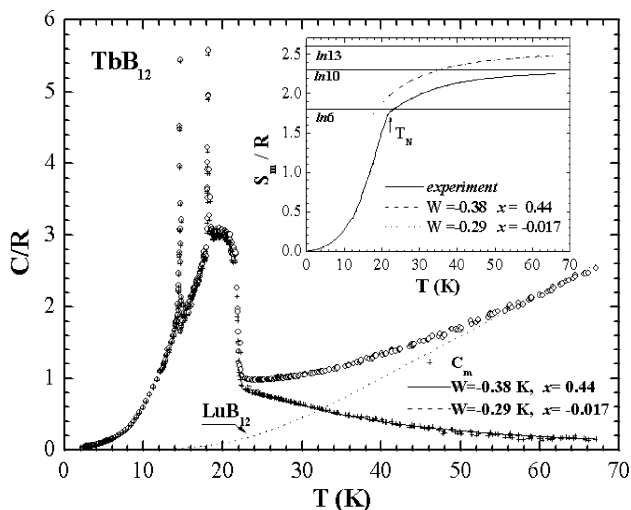


Fig. 3. Temperature dependencies of the full heat capacity  $C_p$ , its magnetic part  $C_m$  and fitting Schottky heat capacities  $C_{\text{Sch}}$  for different  $W$  and  $x$  for  $\text{TbB}_{12}$ . Insert: temperature dependencies of the  $\text{TbB}_{12}$  experimental and calculated entropies.

restricted range of temperatures, where measurements have been done, and with their high temperatures of the magnetic ordering. Therefore, we plan to measure terbium and dysprosium dodecaborides to higher temperatures as well as the heat capacity of their solid solutions with lutetium dodecaboride.

For holmium, erbium and thulium dodecaborides the analysis gives the excellent agreement between the experimental and calculated  $C_{\text{Sch}}$  as well as between the experimental entropy and the calculated one. For illustration the results of such analysis for  $\text{TmB}_{12}$  are shown in Fig. 5. For  $\text{HoB}_{12}$  we obtained  $W = 0.73$  K

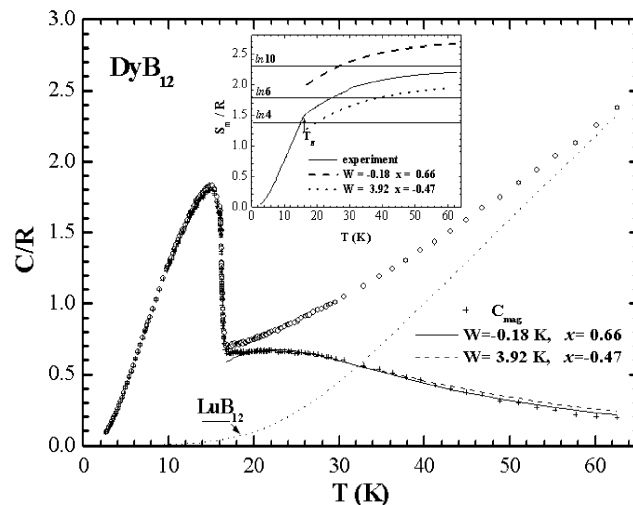


Fig. 4. Temperature dependencies of the full heat capacity  $C_p$ , its magnetic part  $C_m$  and fitting Schottky heat capacities  $C_{\text{Sch}}$  for different  $W$  and  $x$  for  $\text{DyB}_{12}$ . Insert: temperature dependencies of the  $\text{DyB}_{12}$  experimental and calculated entropies.

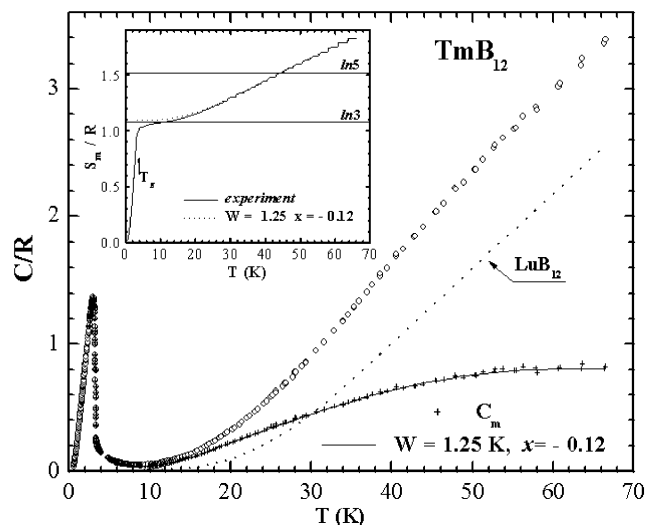


Fig. 5. Temperature dependencies of the full heat capacity  $C_p$ , its magnetic part  $C_m$  and fitting Schottky heat capacity  $C_{\text{Sch}}$  of  $\text{TmB}_{12}$ . Insert: temperature dependencies of experimental and calculated entropies.

and  $x = 0.42$ , which give the triplet  $\Gamma_5^{(1)}$  as the ground state, the doublet  $\Gamma_3^{(1)}$  at 63 K as the first excited level and overall CF-splitting about 420 K; for  $\text{ErB}_{12}$ — $W = -0.85$  K and  $x = 0.37$  and as a consequence the quartet  $\Gamma_8^{(3)}$  as the ground state, the doublet  $\Gamma_6$  at 115 K as the first excited level and the overall splitting about 360 K, and for  $\text{TmB}_{12}$ — $W = 1.25$  K and  $x = -0.12$ , which give the triplet  $\Gamma_5^{(1)}$  as the ground state, the doublet  $\Gamma_3$  at about 80 K and full splitting about 330 K.

For the last three compounds CF parameters  $A_4 \langle r^4 \rangle$  and  $A_6 \langle r^6 \rangle$  are, for sure, negative. The sixth-order term is nearly constant  $[-(22 \pm 4)$  K]. The fourth-order term changes strongly and nearly linearly with the number of the  $4f$ -electrons of REE. Assuming that this behavior holds also for  $\text{TbB}_{12}$  and  $\text{DyB}_{12}$  we have estimated for them new CF parameters. However, they also do not give an agreement with the experiment.

We may compare these CF-parameters with those determined from the Point Charge Model (PCM) [20]. Taking into account five nearest coordination spheres and assuming a charge  $+3|e|$  of RE-ions and  $-2|e|$  of  $\text{B}_{12}$  complexes we obtain the CF-parameters, which are completely different in comparison with the parameters determined from analysis of Schottky heat capacity. First, both terms— $A_4 \langle r^4 \rangle$  and  $A_6 \langle r^6 \rangle$ —are positive and smoothly decreasing with increase of RE atomic number, second, the PCM gives a prevailing contribution from fourth-order term and third—overall CF-splitting does not exceed 35 K.

The PCM is a very crude approximation and the model usually does not work in metallic RE compounds. It is well known that important contribution to the CF arises from interactions with the conduction band: the classical Coulomb's contribution and the exchange contribution. In cubic systems, conduction electrons which have a  $d$ -like character can give a contribution only to the fourth-order CF parameters and those, which have an  $f$ -like character, can give a contribution to the fourth- and sixth-order CF parameters. In a cubic crystal the  $d$ -band is split into  $e_g$  and  $t_{2g}$  sub-bands. The Coulomb interaction depends on the  $e_g$  and  $t_{2g}$  characters of the conduction electrons and these two types of contribution to fourth-order CF parameters have opposite signs. The exchange contribution to the CF parameters keeps the same sign with the  $e_g$  and  $t_{2g}$  electrons. The band structure calculations [2,3] indicate

that the conduction bands in the dodecaborides have mainly  $5d$ -character. One may therefore think that conduction band electrons give a prevailing contribution to crystal field of RE dodecaborides.

According to inelastic neutron scattering experiments on  $\text{Tm}^{11}\text{B}_{12}$  the distances between the ground state and the excited levels are equal to about 83, 160 and 223 K [21] that agrees with our results on CF determination from Schottky heat capacity (Table 2). Also calculated ordered magnetic moment of  $\text{Tm}^{3+}$  ion using CF parameters is in agreement with the experiment [8]. This confirms correctness of the used procedure of CF determination for all  $\text{REB}_{12}$ .

Now we consider the critical region of the antiferromagnetic ordering. We have shown earlier that temperature of the heat capacity maximum  $T_M$  lies below the Néel temperature (Table 1). The second important feature is a magnitude of the heat capacity discontinuity  $\Delta C$  at the antiferromagnetic transition. In the framework of the PFM, the  $\Delta C_{\text{AM}}$  of a system which orders within amplitude-modulated magnetic structure, is equal to  $2/3$  of the  $\Delta C_{\text{EM}}$  expected for a system, which orders within an equal magnetic moment structure.

In the absence of contribution connected with crystal field  $\Delta C_{\text{AM}}$  is described by [14]

$$\Delta C_{\text{AM}}/R = \frac{10}{3} \frac{J(J+1)}{2J^2 + 2J + 1}, \quad (5)$$

where  $J$  is an angular moment.

The first excited CF level in  $\text{HoB}_{12}$ ,  $\text{ErB}_{12}$  and  $\text{TmB}_{12}$  is located too high that practically only the ground state is thermally populated at temperatures near the antiferromagnetic transition. In this case  $\text{HoB}_{12}$  and  $\text{TmB}_{12}$  may be characterized by effective spin  $S_{\text{eff}} = 1$  and  $\Delta C_{\text{AM}} = 11.09$  J/mol K,  $\text{ErB}_{12}$ —by  $S_{\text{eff}} = 3/2$  and  $\Delta C_{\text{AM}} = 12.23$  J/mol K; the experimental  $\Delta C_{\text{AM}}$  values are equal to 10.75, 11.36 and 12.14 J/mol K respectively (Table 3). The agreement is quite good.

In the case of  $\text{TbB}_{12}$  and  $\text{DyB}_{12}$  the Schottky heat capacity at their Néel points is large. This means that excited CF levels are at these temperatures considerably populated. Then for a determination of the  $\Delta C_{\text{AM}}$ , we have to use the more complicated formula given in Ref. [16] which takes into account a full CF splitting. Because of the lack of well-determined CF parameters we have

Table 3  
The most important  $\text{HoB}_{12}$ ,  $\text{ErB}_{12}$ ,  $\text{TmB}_{12}$  characteristics defined from their heat capacity

$\text{REB}_{12}$	$W$ (K)	$x$	The ground state	$A_4 \langle r^4 \rangle$ (K)	$A_6 \langle r^6 \rangle$ (K)	$T_M$ (K)	$\Delta C_{\text{AM}}$ (J/mol K)	
							Experiment	Theory
$\text{HoB}_{12}$	0.73	0.42	$\Gamma_5^{(1)}$	−153.45	−23.61	6.61	10.79	11.08
$\text{ErB}_{12}$	−0.85	0.37	$\Gamma_8^{(3)}$	−118.06	−18.67	6.35	12.14	12.23
$\text{TmB}_{12}$	1.25	−0.12	$\Gamma_5^{(1)}$	−15.51	−25.79	3.06	11.36	11.08

not performed the analysis of the  $\Delta C_{AM}$  in these two compounds.

Nevertheless, it seems nearly sure that all  $4f$ -open shell dodecaborides order within amplitude-modulated magnetic structures. The AM structures in  $TbB_{12}$  [11] and  $TmB_{12}$  [10] have been confirmed by elastic neutron scattering. In the case of the terbium compound the modulation persists well below the lower first-order transition. In this temperature range two magnetic phases, which are described by the same type of propagation vector  $\mathbf{k} = (1/2 \pm \tau, 1/2 \pm \tau, 1/2 \pm \tau)$  but with somewhat different values of  $\tau$  ( $\tau_1 = 0.022$  and  $\tau_2 = 0.059$ ), coexist. The phase transition at 14.6 K is due to the disappearance of additional magnetic phase and the simultaneous rearrangement of the  $\tau$ -components of the  $\mathbf{k}$  vector describing the sine-wave modulation of magnetic moments. In spite of careful examination of neutron data no difference has been found in the temperature range at which the second ( $T_2 = 18.2$  K) first-order transition in heat capacity is observed.

Most likely the terbium compound conserves the sine-wave ordering down to 0 K. Therefore, the CF ground state has to be a nonmagnetic singlet. In fact, the  $\Gamma_2$  singlet ground state we have obtained from an analysis of the Schottky heat capacity. In the other dodecaborides the CF ground state is the magnetic one. Therefore, their AM structures have to be an antiphase at 0 K. Because first-order transition down to temperatures well below their Néel points is not seen; the antiphase structures are reached most likely through the progressive squaring.

Now we analyze the magnetic heat capacity of  $TbB_{12}$ ,  $DyB_{12}$ ,  $ErB_{12}$  and  $TmB_{12}$  well below their Néel temperatures. It contains a nuclear, spin-wave and linear ( $\gamma^*T$ ) terms

$$C = \alpha/T^2 + \gamma^*T + \delta T^3 \exp(-\Delta/T), \quad (6)$$

where  $\Delta$  is an energy gap in a spin-wave spectrum.

Results of this multi-component fitting are shown in Table 4. The nuclear contribution we have found only in  $TbB_{12}$ ; according to it the hyperfine magnetic field  $H_{hf}$  on  $Tb^{3+}$  nucleus is equal to 2.502 MG. An energy gap in spin-wave spectrum for  $TbB_{12}$ ,  $DyB_{12}$  and  $TmB_{12}$  is equal to zero, and one is very small ( $\Delta \approx 0.5$  K) for  $ErB_{12}$ . The energy gap is  $\Delta = (2H_E H_A + H_A^2)^{1/2}$ , where  $H_E$  and  $H_A$  are exchange and magnetocrystalline anisotropy fields, respectively. Therefore, the gapless

spin-wave spectrum means that the magnetocrystalline anisotropy is small.

For all compounds the large linear contribution is obtained. The estimated linear coefficients  $\gamma^*$  are much higher (Table 4) than the electron heat capacity coefficient for the diamagnetic  $LuB_{12}$ — $\gamma = 4.14$  mJ/(mol K<sup>2</sup>). XPS studies of  $TmB_{12}$  [22] have shown that the  $4f$ -shell is well localized and lies 5 eV below the Fermi energy. We may, therefore, expect in this compound as well as in other dodecaborides, a negligible hybridization between  $4f$  and conduction electron states. In consequence there is no enhancement of the electronic heat capacity coefficient  $\gamma$ . Similar phenomenon, i.e. an appearance of the large linear term in the heat capacity of  $UP_xSe_{1-x}$  has been qualitatively explained as a result of the RKKY-type interaction between disoriented magnetic moments [Ref. [23] and references therein].

### 3.2. Thermal expansion

Thermal expansion of magnetic dodecaborides,  $HoB_{12}$ ,  $ErB_{12}$ , and  $TmB_{12}$ , has been measured on single crystals along the  $\langle 001 \rangle$ -axis. The thermal expansion of diamagnetic  $LuB_{12}$  has been analyzed in detail [24], and here we use it as a nonmagnetic reference for the magnetic  $REB_{12}$ .

Since Helmholtz free energy  $F$  of a system is an additive function of free energies of phonons  $F_{ph}$ , conduction electrons  $F_e$  and  $4f$ -electrons  $F_m$  subsystems, the thermal expansion coefficient is

$$\beta = (\partial \ln V / \partial T)_P = -(\partial^2 F / \partial V \partial T) / B_T, \quad (7)$$

where  $B_T$  is the isothermal bulk modulus, is also an additive function of thermal expansion coefficients of corresponding subsystems

$$\beta = \beta_{ph} + \beta_e + \beta_m. \quad (8)$$

The thermal expansion coefficient and heat capacity at constant volume  $C_V$  are related by Grüneisen expression

$$\beta = \gamma_{Gr} C_V / B_T V, \quad (9)$$

where  $C_V$  is the heat capacity at constant volume;  $\gamma_{Gr}$  is the generalized Grüneisen function. A sign of the  $\beta$  is given by a sign of  $\gamma_{Gr}$ .

Table 4

The characteristic values obtained from  $REB_{12}$  heat capacity analyses in ordered range ( $T \leq T_N/4$ )

$REB_{12}$	$\alpha$ (mJ K/mol)	$\gamma^*$ (mJ/mol K <sup>2</sup> )	$\delta$ (mJ/mol K <sup>4</sup> )	$\Delta$ (K)	$H_{hf}$ (MG)
$TbB_{12}$	96	104.4	2.92	0	2.502
$DyB_{12}$	0	73.2	29.38	0	—
$ErB_{12}$	0	130.9	465.0	0.51	—
$TmB_{12}$	0	54.3	1788.0	0	—

The expressions for  $\beta_{\text{ph}}$ ,  $\beta_e$ ,  $\beta_m$  are similar to Eq. (9) but with respective Grüneisen functions ( $\gamma_{\text{ph}}$ ,  $\gamma_e$ ,  $\gamma_m$ ) and heat capacity components ( $C_{\text{ph}}$ ,  $C_e$ ,  $C_m$ ). The generalized Grüneisen function  $\gamma_{\text{Gr}}$  is an average of the individual  $\gamma_r$  weighted by the respective heat capacities  $C_r$ :

$$\gamma_{\text{Gr}} = \frac{\sum_r \gamma_r C_r}{\sum_r C_r} \quad (10)$$

For cubic compounds as in our case  $\beta$  is equal to the triple coefficient of linear thermal expansion  $\alpha$ .

The linear expansion coefficient  $\alpha$  of diamagnetic  $\text{LuB}_{12}$  is a sum only of two components—phonon  $\alpha_{\text{ph}}$  and electron  $\alpha_e$ , and the first one dominates in the studied temperature range. Below 120 K the thermal expansion of this compound has two negative ranges. This behavior is most likely connected with peculiarities of the phonon spectra of the rare earth dodecaborides (Fig. 6) [24].

Temperature dependencies of the linear thermal expansion coefficient  $\alpha$  of  $\text{HoB}_{12}$ ,  $\text{ErB}_{12}$  and  $\text{TmB}_{12}$  are shown in Fig. 6. In the  $\text{ErB}_{12}$  ordered state an extra anomaly of  $\alpha$  occurs at temperature, at which the heat capacity reveals a similar anomaly.

Magnetic contribution to the thermal expansion  $\alpha_m$  we have separated using the thermal expansion of  $\text{LuB}_{12}$  as a nonmagnetic reference with the same factor  $k$  as for heat capacity (Eq. (3)). Determined in such a way the temperature variation of the  $\text{TmB}_{12}$   $\alpha_m$  is shown in Fig. 7. In the paramagnetic state a magnetic contribution to the thermal expansion is determined by CF [25]:

$$\alpha_{\text{CF}} = -\frac{1}{3B_T} \frac{\partial^2 F}{\partial V \partial T} = \frac{1}{3B_T V k_B T^2} \times (\langle E^2 \gamma \rangle - \langle E \gamma \rangle \langle E \rangle), \quad (11)$$

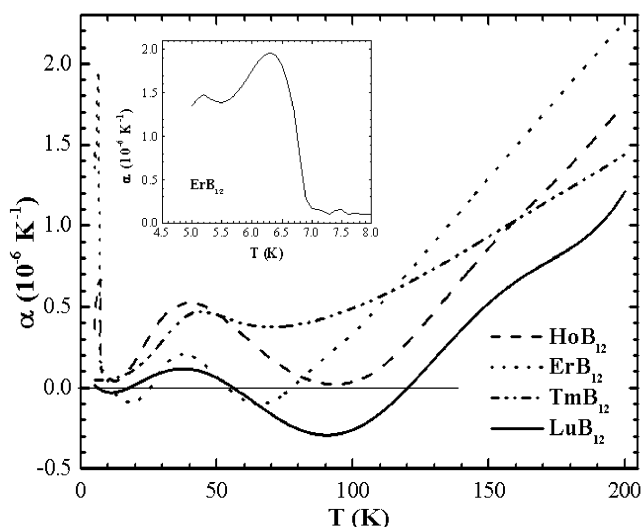


Fig. 6. Temperature dependencies of the thermal expansion coefficients  $\alpha$  for  $\text{REB}_{12}$ . Insert:  $\alpha$  vs.  $T$  for  $\text{ErB}_{12}$  in expanded temperature scale.

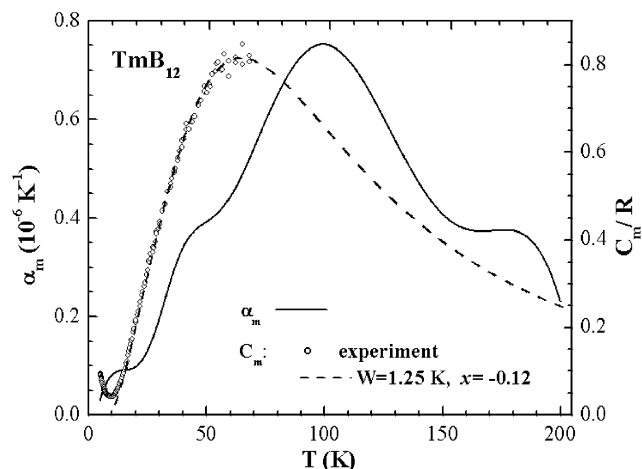


Fig. 7. Temperature dependencies of the magnetic thermal expansion  $\alpha_m$  and magnetic heat capacity  $C_m$  of  $\text{TmB}_{12}$ .

where  $\gamma \equiv \gamma_{\text{CF}}^i = -\partial \ln E_i / \partial \ln V$  is the CF Grüneisen parameter of the CF energy level  $E_i$  with respect to the ground state level.

From comparison of Eqs. (2) and (11) for  $C_{\text{Sch}}$  and  $\alpha_{\text{CF}}$  respectively it is seen that they are proportional when the Grüneisen parameters  $\gamma_{\text{CF}}^i$  for all thermally populated energy levels are the same. For two-level system this requirement is fulfilled automatically.

In Fig. 7 the temperature dependence of the  $\text{TmB}_{12}$  magnetic heat capacities—experimental ( $C_m$ ) and calculated with crystal field parameters ( $C_{\text{Sch}}$ )—are also presented. In paramagnetic region only for  $\text{HoB}_{12}$  the proportionality between  $\alpha_m$  and  $C_{\text{Sch}}$  is observed from 12 up to 100 K, for  $\text{ErB}_{12}$  and  $\text{TmB}_{12}$   $\alpha_m \propto C_{\text{Sch}}$  in a very narrow range—20–30 and 20–40 K, respectively. These three magnetics are multilevel systems (Table 2), so the proportionality between  $\alpha_m$  and  $C_{\text{Sch}}$  is possible only at the above-mentioned conditions: when it may neglect by contribution of second and consequent excited levels or the partial parameters  $\gamma_{\text{CF}}^i$  for all levels are the same.

We have calculated contributions from the individual CF excited levels to Schottky heat capacity to evaluate the temperatures, at which the contribution from each CF level in  $C_{\text{Sch}}$  begins to manifest. For illustration results of calculations are shown for  $\text{TmB}_{12}$  (Fig. 8). It appears that for  $\text{REB}_{12}$  the region of the pseudo two-level system is very narrow and the contribution of the second excited level is necessary to take into account from 15 K for  $\text{HoB}_{12}$ , 20 K for  $\text{ErB}_{12}$  and  $\text{TmB}_{12}$ .

#### 4. Conclusion

1. On the basis of Schottky heat capacity analysis the CF parameters and realistic schemes of CEF levels splitting for RE-ions in  $\text{HoB}_{12}$ ,  $\text{ErB}_{12}$  and  $\text{TmB}_{12}$  are established. The  $\text{RE}^{3+}$  ground states in these

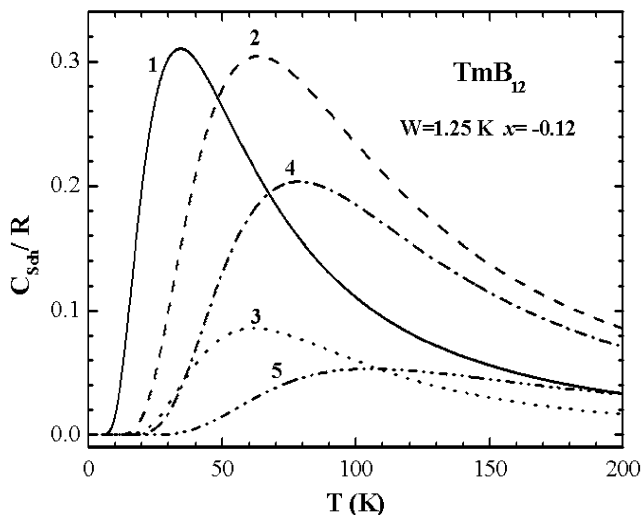


Fig. 8. Temperature dependencies of the individual contributions of CEF excited levels to  $\text{TmB}_{12}$  Schottky heat capacity. Numbers at curves corresponds to transitions from the ground level to 1st, 2nd, etc. excited levels.

compounds ( $\Gamma_5^{(1)}$ ,  $\Gamma_8^{(3)}$  and  $\Gamma_5^{(1)}$  correspondingly) are magnetic and responsible for their magnetic ordering. Apart from the magnetic moment the  $\Gamma_5^{(1)}$  and  $\Gamma_8^{(3)}$  states have also intrinsic quadrupolar moments, which should manifest in magnetic as well as in transport properties of these compounds.

2. CF parameters for  $\text{TbB}_{12}$  and  $\text{DyB}_{12}$  should be taken with caution.

3. Heat capacity behavior in the critical region of  $\text{REB}_{12}$  is characteristic for amplitude-modulated magnetic structure. The first excited CF state of  $\text{HoB}_{12}$ ,  $\text{ErB}_{12}$  and  $\text{TmB}_{12}$  is located so highly that practically only the ground state is thermally populated in the vicinity of the AF transition. The “jump” of the heat capacity  $\Delta C_{\text{AM}}$  at the AF transition, which has been calculated for  $\text{HoB}_{12}$ ,  $\text{ErB}_{12}$  and  $\text{TmB}_{12}$  in the framework of Periodic Field Model, agrees very well with  $\Delta C_{\text{AM}}$  determined experimentally. This fact additionally confirms correctness of the determined CF parameters for these compounds and simultaneously the adequacy of used Periodic Field Model. For  $\text{TmB}_{12}$  and  $\text{TbB}_{12}$  the hypothesis has been confirmed experimentally by elastic neutron study [10,11].

4. Most likely, the amplitude-modulated magnetic structures of  $\text{DyB}_{12}$ ,  $\text{HoB}_{12}$ ,  $\text{ErB}_{12}$  and  $\text{TmB}_{12}$  reach antiphase ones at 0 K through squaring up of the modulation.

5. The small anomaly in the heat capacity of  $\text{ErB}_{12}$  below  $T_N$  most likely is connected with reorientation within the AM structure. Similar effect was observed in other erbium compound— $\text{ErGa}_3$  [26].

6. The magnetic heat capacity analysis for  $\text{TbB}_{12}$ ,  $\text{DyB}_{12}$ ,  $\text{ErB}_{12}$  and  $\text{TmB}_{12}$  at temperatures  $T \leq T_N/4$  revealed suddenly large linear contribution by temperature to  $C_m$ , the nature of which is rather obscure.

7. The  $\text{HoB}_{12}$ ,  $\text{ErB}_{12}$  and  $\text{TmB}_{12}$  magnetic thermal expansion coefficients  $\alpha_m$  demonstrate the complex behavior stipulated in paramagnetic region by CF effect. The proportionality between  $\alpha_m$  and  $C_{\text{Sch}}$  is observed in limited temperature range that is determined by the very narrow region of existence of a pseudo-two-level system.

## References

- [1] H. Bergman (Ed.), Gmelin Handbook of Inorganic Chemistry. Compounds with Boron, Vol. C11a, System 39, Springer, Berlin, Heidelberg, New York, London, Paris, Tokyo, 1990.
- [2] M. Heinecke, K. Winzer, J. Noffke, H. Kranefeld, H. Grieb, K. Flachbart, Yu.B. Paderno, Z. Phys. B 98 (1995) 231.
- [3] N. Okuda, T. Suzuki, I. Ishii, S. Hiura, F. Iga, T. Takabatake, T. Fujita, H. Kadomatsu, H. Harima, Physica B 281&282 (2000) 756.
- [4] L.L. Moiseenko, V.V. Odintsov, J. Less-Common Metals 67 (1979) 237.
- [5] S. Gabani, I. Bat'ko, K. Flachbart, T. Herrmannsdörfer, R. König, Y. Paderno, N. Shitsevalova, J. Magn. Magn. Mater. 207 (1999) 131.
- [6] N. Shitsevalova, Ph.D. Thesis, Institute of Low Temperature and Structure Research, Wrocław, 2001 (in Russian).
- [7] B.T. Matthias, T.H. Geballe, K. Andres, E. Corenzwitt, G.W. Hull, J.P. Maita, Science 159 (1968) 530.
- [8] P.C.M. Gubbens, A.M. van der Kraan, K.H.J. Bushow, Physica B 130 (1985) 412.
- [9] K.R. Lea, M.J.M. Leask, W.P. Wolf, J. Phys. Chem. Solids 23 (1962) 1381.
- [10] A. Czopnik, A. Murasik, L. Keller, N. Shitsevalova, Y. Paderno, Phys. Stat. Sol. (b) 221 (2000) R7.
- [11] A. Murasik, A. Czopnik, L. Keller, M. Zolliker, N. Shitsevalova, Y. Paderno, Phys. Stat. Sol. (b) 234 (2002) R13–R15.
- [12] A. Murasik, A. Czopnik, E. Clementyev, S. Janssen, N. Shitsevalova, Phys. Stat. Sol. (b), in print.
- [13] J.A. Blanco, D. Gignoux, P. Morin, D. Schmitt, J. Magn. Magn. Mater. 90 (1990) 166.
- [14] J.A. Blanco, D. Gignoux, D. Schmitt, Phys. Rev. B 43 (1991) 13145.
- [15] J.A. Blanco, D. Gignoux, D. Schmitt, Phys. Rev. B 45 (1992) 2529.
- [16] J.A. Blanco, D. Schmitt, J.C. Gomez Sal, J. Magn. Magn. Mater. 116 (1992) 128.
- [17] Yu. Paderno, V. Filippov, N. Shitsevalova, in: D. Emin, T.L. Aselage, et al. (Eds.), Boron-Rich Solids, AIP Conference Proceedings, Vol. 230, Albuquerque, 1991, p. 460.
- [18] A.I. Krivchikov, B.Ya. Gorodilov, A. Czopnik, in: Proceedings of the Conference on Low Temperature Thermometry and Dynamic Temperature Measurement, Wrocław, 1997, p.V7.
- [19] G. Brandli, R. Griessen, Cryogenics 13 (1973) 299.
- [20] M.T. Hutchings, Solid State Phys. 16 (1964) 227.
- [21] A. Murasik, A. Czopnik, N. Shitsevalova, Y. Paderno, L. Keller, in: IAE Annual Report 1999, Otwock-Swierk, Poland, 1999, p. 69.
- [22] F. Iga, Y. Takakuwa, T. Takahashi, M. Kasaya, T. Kasuya, T. Sugawa, Solid State Commun. 50 (1984) 903.
- [23] A. Blaise, J.E. Gordon, R. Lagnier, M. Mortimer, R. Troc, J. Magn. Magn. Mater. 38 (1983) 109.
- [24] A. Czopnik, N. Shitsevalova, A. Pietraszko, V. Pluzhnikov, Yu. Paderno, A. Krivchikov, J. Alloys. Comp., in print.
- [25] T.H.K. Barron, J.G. Collins, G.K. White, Adv. Phys. 29 (1980) 609.
- [26] A. Murasik, A. Czopnik, L. Keller, P. Fischer, J. Magn. Magn. Mater. 213 (2000) 101.